Pristine and iron-engineered animal- and plant-derived biochars enhanced bacterial abundance and immobilized arsenic and lead in a contaminated soil

He Pan [a,1], Xing Yang [b,c,1], Hanbo Chen [b,d], Binoy Sarkar [e], Nanthi Bolan [f], Sabry M. Shaheen [c,g,h], Fengchang Wu [i], Lei Che [j], Yibing Ma [k], Jörg Rinklebe [c,l], Hailong Wang [a,b,*]

[a] Key Laboratory of Soil Contamination Bioremediation of Zhejiang Province, School of Environmental and Resource Sciences, Zhejiang A&F University, Hangzhou, 311300, China

[b] Biochar Engineering Technology Research Center of Guangdong Province, School of Environmental and Chemical Engineering, Foshan University, Foshan, 528000, China

[c] University of Wuppertal, School of Architecture and Civil Engineering, Institute of Foundation Engineering, Water- and Waste-Management, Laboratory of Soil- and Groundwater-Management, Pauluskirchstraße 7, 42285 Wuppertal, Germany

[d] Agronomy College, Shenyang Agricultural University, Shenyang, 110866, China

[e] Lancaster Environment Centre, Lancaster University, Lancaster, LA1 4YQ, United Kingdom

[f] The Global Centre for Environmental Remediation, University of Newcastle, Callaghan, NSW, Australia

[g] King Abdulaziz University, Faculty of Meteorology, Environment, and Arid Land Agriculture, Department of Arid Land Agriculture, 21589 Jeddah, Saudi Arabia

[h] University of Kafrelsheikh, Faculty of Agriculture, Department of Soil and Water Sciences, 33516, Kafr El-Sheikh, Egypt

[i] State Key Laboratory of Environmental Criteria and Risk Assessment, Chinese Research Academy of Environmental Sciences, Beijing, 100012, China

[j] School of Engineering, Huzhou University, Huzhou, 313000, China

[k] Macau Environmental Research Institute, Macau University of Science and Technology, Macau, 999078, China

[l]Department of Environment, Energy and Geoinformatics, Sejong University, Seoul 05006, Korea

[1] These authors contributed equally to this work and should be considered co-first authors.

*Corresponding author. E-mail: hailong.wang@fosu.edu.cn

Abstract

In this study, typical animal- and plant-derived biochars derived from pig carcass (PB) and green waste (GWB), and their iron-engineered products (Fe-PB and Fe-GWB) were added at the dose of 3% (w/w) to an acidic (pH = 5.8) soil, and incubated to test their efficacy in improving soil quality and immobilizing arsenic (As = 141.3 mg kg^{-1}) and lead (Pb = 736.2 mg kg^{-1}). Soil properties, microbial activities, and the geochemical fractions and potential availabilities of As and Pb were determined in the non-treated (control) and biochar-treated soil. Modification of PB (pH = 10.6) and GWB (pH = 9.3) with Fe caused a decrease in their pH to 4.4 and 3.4, respectively. The application of PB and GWB significantly increased soil pH, while Fe-PB and Fe-GWB decreased soil pH, as compared to the control. Application of Fe-GWB and Fe-PB decreased the $NH_4H_2PO_4$-extractable As by 32.8 and 35.9%, which was more effective than addition of GWB and PB. However, PB and GWB were more effective than Fe-PB and Fe-GWB in Pb immobilization. Compared to the control, the DTPA-extractable Pb decreased by 20.6 and 21.7%, respectively, following PB and GWB application. Both biochars, particularly PB significantly increased the 16S rRNA bacterial gene copy numbers, indicating that biochar amendments enhanced the bacterial abundance, implying an alleviation of As and Pb bio-toxicity to soil bacteria. The results demonstrated that pristine pig carcass and green waste biochars were more effective in immobilizing Pb, while their Fe-engineered biochars were more effective in As immobilization in co-contaminated soils.

Keywords: Modified biochar; biomass waste treatment; heavy metals; soil remediation; soil microbial community.

1. Introduction

In recent decades, soil contamination with potentially toxic elements (PTEs), such as arsenic (As) and lead (Pb), has been considered as a public and environmental health concern (Shaheen et al., 2017; Bandara et al., 2020). Appropriate soil remediation trials are urgently needed to mitigate the potential risks and threats of PTEs to the soil ecosystem and human health (Antoniadis et al., 2017). Soil amendments have been commonly used for *in situ* remediation of soils contaminated by PTEs (Lu et al., 2014; Wang et al., 2020; Palansooriya et al., 2020). For example, organic and inorganic amendments such as biochar and iron (Fe) materials have been used to immobilize PTEs in soil by transforming the elements into less mobile and non-available fractions (Wang et al., 2020; Wu et al., 2020).

Biochar has extensively been applied to purify wastewater (Fang et al., 2020; Lu et al., 2020; Yin et al., 2020), and to mitigate the environmental risks presented by soils contaminated with PTEs (e.g., Nie et al., 2018; Beiyuan et al., 2020; Rinklebe et al., 2020). The performance of biochar for PTEs immobilization is based on its favorable properties, including highly porous structure, large surface area, and abundance of various functional groups (Bandara et al., 2020; Li et al., 2020; Tang et al., 2020). In addition, the efficiency of biochar for PTE immobilization widely depends on the element type (Yang et al., 2017; Chen et al., 2020). For instance, Yang et al. (2017) applied 5% tobacco stalk biochar to a soil dual-contaminated by Cd and Zn, they reported the concentrations of extractable Cd and Zn respectively reduced by 64.2 % and 94.0%. Studies indicated that pristine biochar often exhibits relatively lower sorption/immobilization efficiency than engineered/modified biochar (Li et al., 2019; Shaheen et al., 2019; Amen et al., 2020). Therefore, a chemical modification has been suggested in order to improve the sorption/immobilization capacity of biochar (Kwon et al., 2020; Panahi et al., 2020). Iron materials have high sorption ability for PTEs (Komarek et al., 2013; Qiao et al., 2019). Recently, different types of iron-engineered plant-derived biochars have been developed and used for soil and groundwater remediation (e.g., Lu et al., 2018; Xia et al., 2019; Wan et al., 2020). However, to our best knowledge, limited research has been directed to determine the effect of Fe-engineered animal-derived biochar on immobilization of anionic (e.g., As) and cationic (e.g., Pb) toxic elements in co-contaminated soils.

The potential mobility, bioavailability and toxicity of PTEs are closely related with the total concentration, and their geochemical binding forms present in the soil (Lu et al., 2017). The soluble and exchangeable forms of PTEs in soils are considered to be representative of their mobility, bioavailability and toxicity (Yang et al., 2017), which biochar could alter following application to contaminated soils.

Furthermore, microbial activities are sensitive to the change of soil properties, especially to the toxicity of soil contaminants, which have been widely used for soil health monitoring (Xia et al., 2019; Tang et al., 2020). Previous studies have shown that the application of biochar could mitigate the stress from PTEs, and improve the abundance of microorganisms in PTE-contaminated soils through providing various nutrients and appropriate habitat (e.g., Xu et al., 2018; Xing et al., 2019; El-Naggar et al., 2020). However, there is still a lack of information on the influence of Fe-engineered biochar on microbial activities in As and Pb co-contaminated soils. The study of As and Pb in biochar-amended soils warrants special attention because of the sensitivity of both elements to the dynamic redox conditions of soils often undergoing intermittent water-logging which is a well-known factor for controlling elemental speciation and fractionation.

We hypothesize that Fe-engineered biochar could synthesize merits of both biochar (high sorption capacity for cations, e.g., Pb^{2+}) and iron oxides (high sorption capacity for AsO_4^{3-}) in decreasing the bioavailability of As/Pb by altering their redistribution, and changing the microbial activity in a co-contaminated soil. To test this hypothesis, we aimed to: (1) determine the impact of pristine and Fe-engineered pig carcass and green waste-derived biochar on the physiochemical properties, gene abundance of bacteria and fungi, and geochemical fractions and bioavailability of As and Pb in co-contaminated soil, and (2) assess the impact of Fe loading process on the immobilization efficiency of both studied biochars and their feasibility for the remediation of As and Pb co-contaminated soil.

2. Materials and methods

2.1 Soil sampling and characterization

A top-soil (0-20 cm) was collected from a paddy field in Shangyu City, Zhejiang Province, China (30°00′N, 120°79′E). The sampling site was adjacent to a Pb/Zn mine tailing, and the soil was co-contaminated with As and Pb. The total concentration of As (141.3 mg kg^{-1}) and Pb (736.2 mg kg^{-1}) exceeded the risk screening level according to the Soil Environmental Quality Standard GB 15618–2018 (30 mg kg^{-1} for As, and 100 mg kg^{-1} for Pb). The soil texture was classified as a silty clay loam soil as per the Food and Agricultural Organization (FAO) system. The soil sample was air-dried, ground, and sieved through a 3-mm stainless steel screen prior to the incubation experiment. Key soil properties, i.e., pH, cation exchange capacity (CEC), electrical conductivity (EC), available P, and particle size distribution were characterized as per standard methods (Lu et al., 2014). Total As and Pb concentration in the soil was extracted by digesting the soil in HF-$HClO_4$-HNO_3 (Yang et al., 2016), and quantified by Inductively Coupled Plasma Optical Emission Spectroscopy (ICP-OES, Optima 2000, PerkinElmer Co., USA). The quality control for total As and Pb analysis in soil samples was confirmed by analyzing appropriate reagent blanks, certified reference soil (GBW-07405; State Technology Supervision Administration, China), and commercially available standard (Soil Environmental Quality Standard). The recoveries of As and Pb in the analysis method were 104.5 and 96.5%, respectively. Selected physicochemical properties of the experimental soil are provided in Table 1.

2.2 Biochar preparation, iron-engineering, and characterization

Green waste biochar (GWB) and pig biochar (PB) were produced from smashed (5 mm) branches of *Platanus orientalis* Linn. and whole dead pig carcasses, respectively. The raw materials were pyrolyzed under oxygen-limited conditions for 2 h at a peak temperature of 650°C. The GWB and PB were ground, and sieved to pass a 2-mm screen prior to use.

To prepare Fe-engineered biochars, sieved GWB and PB were added to a $FeCl_3 \cdot 6H_2O$ solution at a biochar to Fe mass ratio of 20:1, and then sonicated for 1 h at 25°C. Subsequently, the Fe-soaked GWB/PB were oven-dried at 60°C until attaining a constant weight. Finally, the Fe-soaked biochars were

subjected to pyrolysis again at 650°C for 1 h (Dong et al., 2016). The Fe-engineered biochars were named as Fe-GWB and Fe-PB.

The concentrations of As and Pb in biochar were measured using HNO_3-HF-$HClO_4$ digestion method, and quantified by ICP-OES (Yang et al., 2016). The specific surface area (SSA) of the biochar was determined by Brunauer-Emmett-Teller (BET) N_2 adsorption analysis at 77 K on a surface area analyzer (TristarII3020, Micromeritics Instrument Corporation, USA) after degassing (Lu et al., 2014). The functional groups of the biochars were analyzed by Fourier transform infrared (FTIR) spectrometer (Nicolet iS10, ThermoFisher, USA) following KBr disc sample preparation method (Yang et al., 2016). The morphology and porous structure of biochars were examined using a scanning electron microscope (SEM) (Sirion-100, FEI, Poland). The energy dispersive X-ray spectrometry (EDS) was used for the elemental analysis of biochar particles. Selected properties of the biochar samples are provided in Table 1. More details about the experimental soil and biochar properties are given in Supplementary Material (Table S1).

Table 1 Selected physicochemical properties of the biochars and experimental soil.

Properties	GWB	PB	Fe-GWB	Fe-PB	Soil
C (%)	69.3	30.8	59.9	40.4	-
H (%)	2.7	1.3	2.2	1.5	-
N (%)	1.1	2.1	0.9	1.8	-
pH	9.3	10.6	4.4	3.6	5.8
Electrical conductivity (dS m^{-1})	0.4	2.0	4.5	4.3	0.05
Cation exchange capacity (cmol kg^{-1})	21.6	16.7	4.7	6.4	13.4
Ash (%)	6.6	60.0	15.8	76.3	-
Specific surface area (m^2 g^{-1})	110.7	18.4	74.5	43.6	-
Surface alkalinity (cmol kg^{-1})	215.9	245.7	183.6	227.6	-
Total P (g kg^{-1})	1.9	81.3	3.0	70.7	-
Total Pb (mg kg^{-1})	7.0	1.6	11.4	4.6	736.2
Total As (mg kg^{-1})	ldl	ldl	ldl	ldl	141.3
Total Fe (g kg^{-1})	7.6	20.6	54.6	62.3	-
Olsen P (mg kg^{-1})	nd	nd	nd	nd	1.82
Sand (%)	nd	nd	nd	nd	33.5
Silt (%)	nd	nd	nd	nd	45.8
Clay (%)	nd	nd	nd	nd	20.6

GWB: green waste biochar; PB: pig biochar; Fe-GWB: Fe-engineered green waste biochar; Fe-PB: Fe-engineered pig biochar; ldl: lower than detection limits; nd: not determined.

2.3 Experimental design

An incubation experiment was conducted in a randomized block design with 800 g of soil sample amended with 24 g of raw or Fe-engineered biochar (3%, w/w), mixed well, and placed into a plastic pot (11 cm in diameter, 15 cm in height). Soil receiving no biochar served as the control. Four replicates were run for each treatment. All pots were watered with deionized water to maintain 70% of the soil's water holding capacity, and placed in a greenhouse at 25°C. Equal volume of deionized water was added to all pots when small cracks started to appear on the soil surface indicating water deficit, to simulate an alternatively wet and dry dynamic process. After 30 days of incubation, soil samples were retrieved from each pot. Soil sub-samples were air-dried at room temperature, and ground to pass 2-mm sieve for further analyses, including soil pH, TOC, the available As and Pb concentrations, sequential extraction of As and Pb, and the abundance of bacteria and fungi. Another sub-sample was immediately stored at -70°C freezer after freeze-drying for the soil enzymatic activity and microbial community structure analyses.

2.4 Soil analysis

For the measurement of potentially available Fe and Pb in the soil, 5 g of air-dried soil (2 mm) was weighed into a plastic centrifuge tube, shaken with 25 mL 0.005 M diethylenetriaminepentaacetic acid (DTPA) solution (pH 7.3) for 2 h, centrifuged at 3000 rpm for 10 min, and then the supernatant was filtered through a 0.45-μm membrane filter before analysis on ICP-OES (Lindsay and Norvel, 1978). For the extraction of potentially available As in soil, 1 g of air-dried soil (2 mm) was weighed into a 50-mL plastic centrifuge tube, shaken with 25 mL $NH_4H_2PO_4$ (0.05 M) at 250 rpm for 16 h at 20°C. Afterwards, the mixture was centrifuged at 3000 rpm for 15 min. Thereafter, the supernatant was filtered through a 0.45-μm membrane filter before measured with ICP-OES (Wenzel et al., 2001). Key physicochemical properties (pH, TOC and Olsen P) of the control and biochar-amended soils were determined using standard methods (Yang et al., 2016; Nie et al., 2018).

2.5 Sequential extraction of As and Pb

The geochemical fractions of As were sequentially extracted according to the method described by Wenzel et al. (2001). Based on the extraction method, the five fractions of As in the soils corresponded to non-specifically adsorbed As (As_{nsa}), specifically adsorbed As (As_{sa}), amorphous Fe/Mn oxides bound As (As_{am}), crystalline Fe/Mn oxides bound As (As_{cr}), and residual As (As_{re}). A five-step sequential extraction method was used to extract the geochemical fractions of Pb in the non-treated and biochar-treated soils (Tessier et al., 1979). The extracted fractions of Pb were exchangeable Pb (Pb_{ex}), carbonate bound Pb (Pb_{ca}), Fe/Mn oxide bound Pb ($Pb_{Fe/Mn}$), organic bound Pb (Pb_{or}), and residual Pb (Pb_{re}). The concentrations of As and Pb in various fractions as extracted by the above methods and in digested liquids were measured by ICP-OES following filtering through 0.45-μm membrane.

2.6 DNA extraction and real-time quantitative PCR

DNA was extracted from the soil samples (2 mm, 0.35 g) using the Power Soil DNA Isolation Kit (MoBio Labories, Carlsbad, CA, USA) following the instructions of the manufacturer. The quantity and quality of the extracted DNA were determined using a NanoDrop spectrophotometer (NanoDrop Technologies, ND-1000, USA). The extracted DNA was stored at -20°C for further analyses.

The 16S rRNA genes of the bacteria, and 18S rRNA genes of the fungi were amplified. Amplification libraries were prepared with labeled universal primers for bacteria and fungi, i.e., 338F and 518R for bacteria (Fierer et al., 2005), and NSIF and FungR for fungi (May et al., 2001; Xu et al., 2020), respectively. Each of the DNA sample was amplified separately using the fusion primer pair 338F (5′-ACTCCTACG-GGAGGCAGC-3′) and 518R (5′-ATTA-CCGCGGCTGCTGG-3′) for bacteria, and NSIF (5′-GTAGTCATATGCTTGTCTC-3′) and FungR (5′-ATTCCCCGTTACCCCTTG-3′) for fungi to obtain quantitative analysis. Real-time quantitative PCR (qPCR) reactions were performed in 10 μL of TB Green™ Premix Ex Taq™ (TAKARA BIO INC, China), 0.5 μL of each primer, 1 μL of template DNA, and 8 μL of ultrapure sterile water. The real-time qPCR reaction conditions of bacterial 16S rRNA were consisted of: pre-denatured at 94°C for 2 min, denatured for 30 s, annealed at 55°C for 30 s, pre-extended at 72°C for 30 s, the above steps repeated for 35 times, and extended at 72°C for 5 min (Fierer et al.,

2005). Compared to bacteria, the reaction conditions of qPCR of fungi were 1 min longer in pre-denaturation, 2°C higher in annealing temperature, and 10 s longer in pre-extension step (May et al., 2001). A standard curve was generated using 10-fold serial dilutions of plasmids containing bacterial 16S rRNA gene and fungal 18S rRNA region from environmental samples (Chen et al., 2013; Xu et al., 2021). The real-time qPCR runs were setup, data collected, and analyzed with a CFX96^{TM} Real-Time PCR System (CFX96^{TM} Optics Module, Singapore).

2.7 Statistical analysis

The SPSS 17.0 statistical package (IBM, USA) was used to perform statistical analysis of the data. One-way analysis of variance (ANOVA) and Tukey multiple comparison tests were used to assess the statistical difference of soil pH, TOC, available As and Pb concentrations, and the abundance of bacteria and fungi among the treatments. The variability in the data was expressed as standard error, and the level of significance was set at $P<0.05$. The correlation matrix was based on the Pearson's correlation coefficients ($P<0.05$).

3. Results and discussion

3.1 Characteristics of the pristine and iron-engineered biochars

The pH of Fe-GWB (4.41) and Fe-PB (3.57) were lower than GWB (9.25) and PB (10.56) (Table 1). This means that the Fe-loading process caused a significant decrease of pH, which could be due to the release of a high amount of H^+ due to the hydrolysis of Fe from the Fe-engineered biochars (Yin et al., 2017). The iron-engineered biochars had a higher salt content than the raw biochars as indicated by the EC values (Table 1), which could be attributed to the exogenous Cl^- and Fe^{3+} from the Fe-loading process. The ash content, total P, and surface alkalinity of PB and Fe-PB were higher than those of GWBs (Table 1). The SSA of Fe-GWB (74.47 $m^2 g^{-1}$) was lower than that of GWB (110.70 $m^2 g^{-1}$), while Fe-PB (43.6 $m^2 g^{-1}$) had a higher SSA than PB (18.4 $m^2 g^{-1}$) (Table 1). The SEM image showed more apparent porous structure of GWBs than that of PBs (Fig. S1). The concentrations of total Fe in the Fe-engineered

biochars were higher than the pristine biochars (Table 1), which proved that Fe compounds were loaded onto the biochar due to the modification, as also confirmed by the EDS spectra (Fig. S2).

The FTIR spectra (Fig. 1) indicated that the specific bands at 550 to 1000 cm^{-1}, and 1050 cm^{-1} were stronger in the spectra of PB and Fe-PB than those of GWB and Fe-GWB, indicating that PBs contained more functional groups than GWBs. These bands represented olefin (650-1000 cm^{-1}) and C-O-C (1050 cm^{-1}) groups, as also reported in other studies (e.g., Wu et al., 2012; Fang et al., 2014). Compared to PB, the intensity of C-O-C (1050 cm^{-1}) band in Fe-PB was increased. However, the intensity of some bands (e.g., C=C (1448-1576 cm^{-1}) and C=O (1480 cm^{-1})) decreased in Fe-GWB, as compared to GWB, which was likely due to the decomposition of chemical substances and breaking of double bonds during the second-time pyrolysis (Wan et al., 2020).

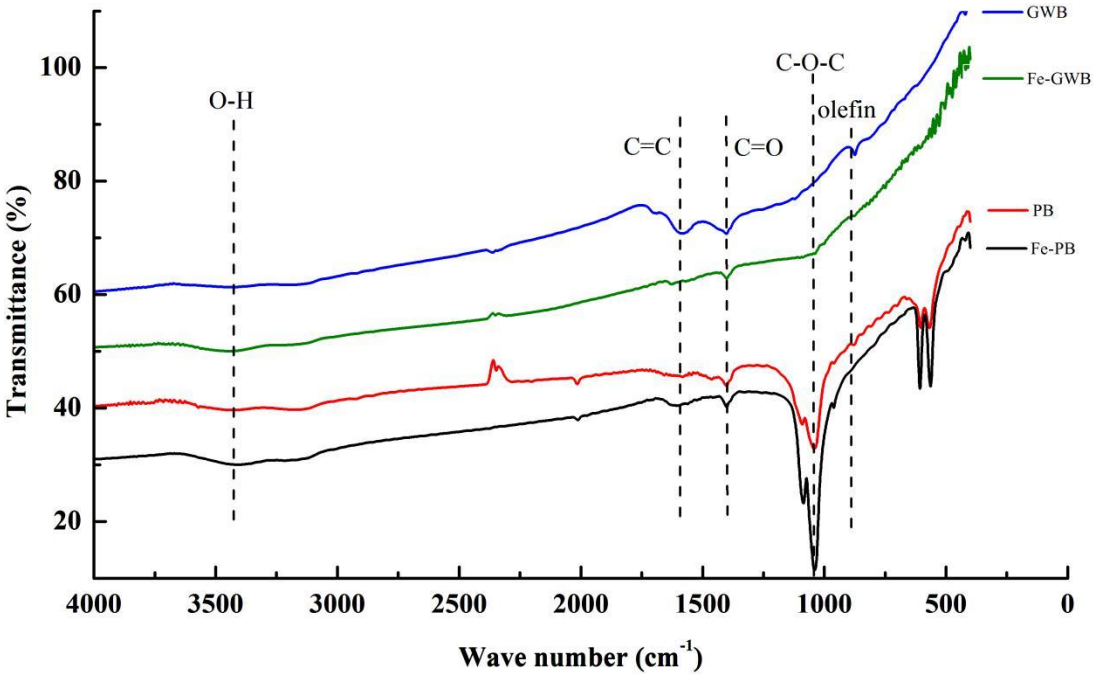

Fig. 1 Fourier transform infrared (FTIR) spectra of green waste biochar (GWB), pig biochar (PB), iron-engineered green waste biochar (Fe-GWB), and iron-engineered pig biochar (Fe-PB).

3.2 Effect of biochars on pH and TOC of soil

The soil pH increased by 1.3 and 1.3 units with the addition of GWB and PB, whereas decreased by 1.1 and 0.7 units with the addition of Fe-GWB and Fe-PB, respectively, compared to the control (Fig.

2A). The change of soil pH could be attributed to the direct influence of the amendments of the pristine and modified biochars with contrasting pH. The Fe-engineered biochars had lower pH values than pristine biochars (Table 1), which could decrease the soil pH. The release of hydrogen ions (H^+) caused by Fe^{3+} hydrolysis might be another reason for the reduction of soil pH in Fe-engineered biochar treatments, as also reported by Yin et al. (2017).

As compared to the control, the TOC significantly (P<0.05) increased by 159.3, 53.7, 153.7, and 35.5%, in the soils treated with GWB, PB, Fe-GWB and Fe-PB, respectively (Fig. 2B), which was in consistence with the carbon content in the biochars (Table1). The effect of GWB was more effective than that of PB in increasing soil TOC, which could be due to the relatively higher C content in GWB than PB (Table 1).

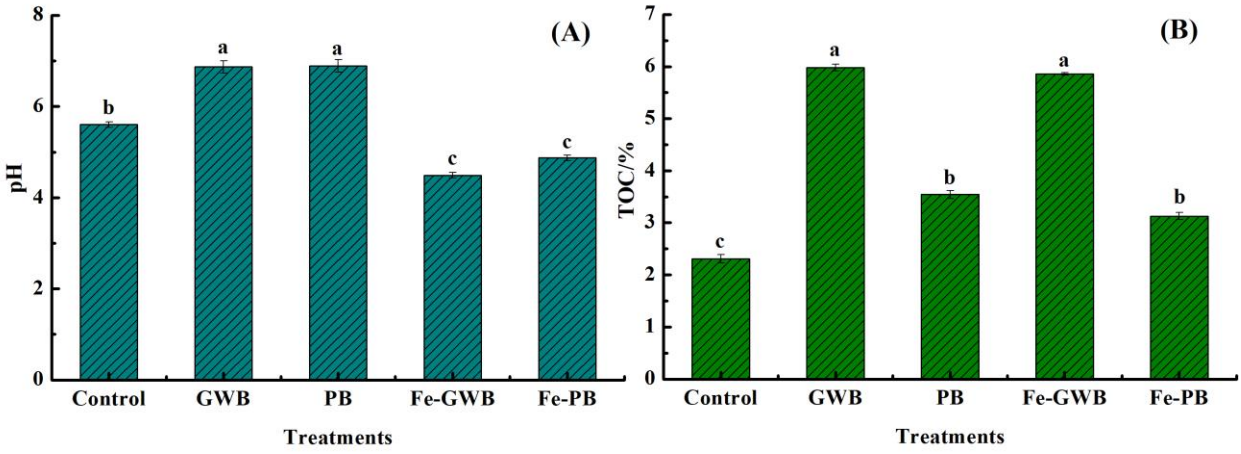

Fig. 2 Effect of pristine and iron-engineered biochar application on soil pH (A), and total organic carbon (TOC) (B). Treatments: green waste biochar (GWB), pig biochar (PB), iron-engineered green waste biochar (Fe-GWB), and iron-engineered pig biochar (Fe-PB). Error bars are standard error of the mean (n=4). Different letters above the bars indicate significant difference between treatments at P<0.05.

3.3 Effect of biochars on the fractionation and bioavailability of As

The soluble + exchangeable forms of metal(loid)s are considered to be mobile and bioavailable, thus are frequently employed to assess the biotoxicity and bioavailability of metal(loid)s in soil (Bandara et al., 2020). Compared to the control, the $NH_4H_2PO_4$-extractable As (bioavailable As) in the soil amended with

Fe-GWB and Fe-PB decreased by 32.8 and 35.9%, respectively (Fig. 3A). Application of the pristine biochars had no significant influence on the bioavailable As in soil, compared to the control (Fig. 3A).

Arsenic was mainly distributed in the Fe oxide fractions (As_{cr} and As_{am}), followed by the residual, specifically adsorbed, and non-specifically adsorbed fractions in all treatments (Fig 3B). Addition of GWB and PB reduced the proportion of As_{nsa} from 1.5% to 0.6% and 0.3%, respectively. Application of Fe-GWB and Fe-PB effectively decreased the mobile fraction of As (sum of As_{nsa} and As_{sa}) from 5.0 to 2.7 and 3.1%, respectively; while Fe-GWB increased the residual fraction from 17.9 to 20.4%, as compared to the control (Fig. S3), indicating that the Fe-engineered biochars could promote the transfer of As from mobile fractions to stable fractions. The Fe-engineered biochars were more effective than the pristine biochars in transforming As to relatively stable fractions.

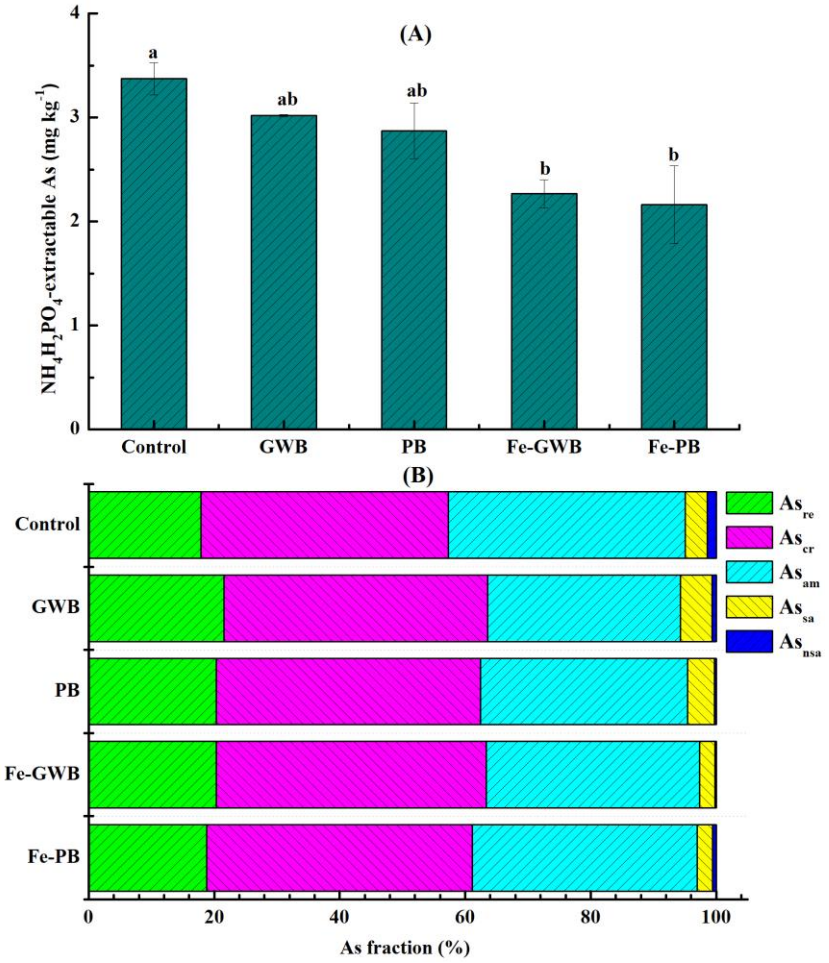

Fig. 3 Effect of pristine and iron-engineered biochar application on $NH_4H_2PO_4$-extractable As (A), and redistribution of As (B) in the soil. Treatments: green waste biochar (GWB), pig biochar (PB), iron-engineered green waste biochar (Fe-GWB) and iron-engineered pig biochar (Fe-PB). As fractionation: Non-specifically adsorbed As (As_{nsa}), specifically adsorbed As (As_{sa}), amorphous Fe-Mn oxide bound As (As_{am}), crystalline Fe-Mn oxide bound As (As_{cr}), and residual As (As_{re}). Error bars are standard error of means (n=4). Different letters above bars indicate significant difference between treatments at $P<0.05$.

pH is a crucial factor which affects the release of As from soil through altering the surface charge of soil particles (Karczewska et al., 2018). The decrease of $NH_4H_2PO_4$-extractable As, and As_{nsa} and As_{sa} fractions after addition of the Fe-engineered biochars (Fig. 3A,B) might be attributed to the decrease of soil pH (Fig. 2A), which might lead to an increase of positive charge on soil particles, thus enhancing immobilization of anionic As through electrostatic adsorption. In addition, the functional groups on the Fe-engineered biochars, including -NH, -OH and -COOH (Fig. 1), could be protonated under low pH, reducing As mobilization through the formation of stable complexes between the negatively charged As ions and positively charged functional groups (Shaheen et al., 2019; Lu et al., 2020). Bolan et al. (2013) also found that low soil pH increased the positive charge on soil colloids, and kept As in relatively stable form through electrostatic attraction.

The exogenous Fe and organic carbon generated from the Fe-engineered biochars could form complexes with As to promote As fixation. Iron oxides mainly affect the fractionation of As in soil, and which could enhance the ability of soil to immobilize As (Shaheen et al., 2017; El-Naggar et al., 2020). Iron oxides and hydroxides had strong As adsorption capacity through electrostatic and chemical adsorptions (Wan et al., 2020). Therefore, the low concentration of $NH_4H_2PO_4$-extractable As, and the small proportion of As_{nsa} and As_{sa} in Fe-engineered biochar-treated soils could be attributed to the exogenous Fe materials applied via Fe-engineered biochar. Arsenic anions such as AsO_4^{3-} and $HAsO_3^{2-}$ could be immobilized by Fe oxides via co-precipitation and adsorption (Han et al., 2019). High concentration of phosphate in soil might compete with As anions for surface binding sites, thereby increasing the mobilization of As (Zeng et al., 2012). However, despite high Olsen-P was observed in PB treatment in this study (Table S1), no significant difference in $NH_4H_2PO_4$-extractable As concentrations

between control and PB-treated soil was observed (Fig. 3A). This result indicated that phosphate played a less important role than iron oxides in affecting the extractability of As in the studied soil. Pearson's correlation analysis showed no significant correlation between Olsen-P and $NH_4H_2PO_4$-extractable As concentrations (Fig. 4). These results demonstrated that the modification of PB and BWB with Fe materials increased their ability for As immobilization.

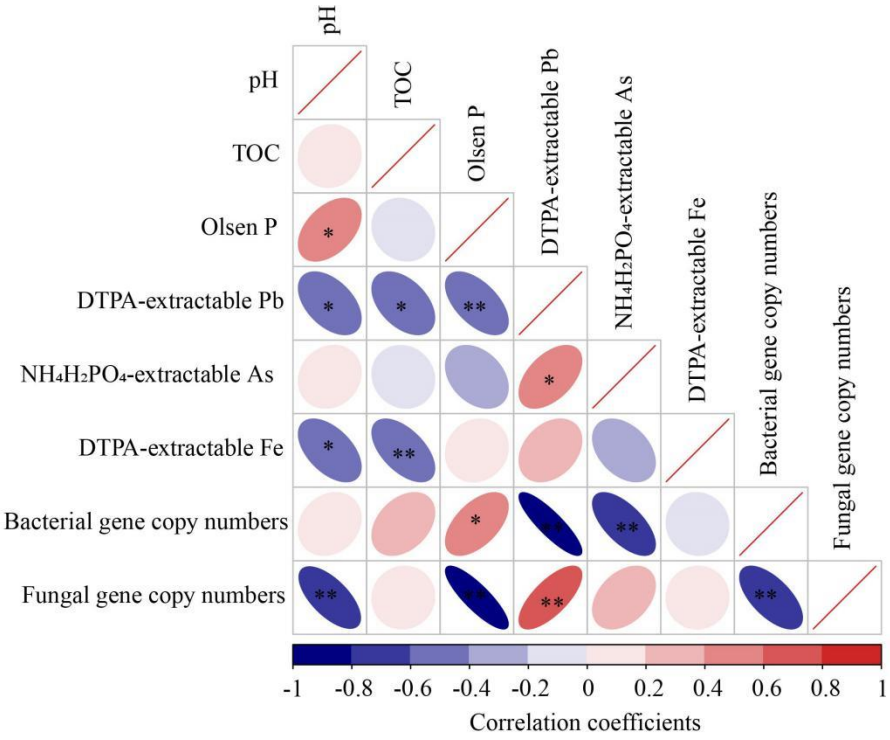

Fig. 4 Pearson's correlation matrix featuring relationships between $NH_4H_2PO_4$-extractable As, DTPA-extractable Pb and other parameters. Note: ** Correlation is significant at the 0.01 level; * Correlation is significant at the 0.05 level.

3.4 Effect of biochars on the fractionation and bioavailability of Pb

The concentration of DTPA-extractable Pb (bioavailable Pb) in soil significantly (P<0.05) decreased in all biochar treatments and pristine biochars were more effective than Fe-engineered biochars in decreasing the DTPA-extractable Pb concentration, with a decrease of 20.6, 21.7, 12.1 and 15.5% for GWB, PB, Fe-GWB and Fe-PB, respectively, as compared to the control (Fig. 5A).

The Pb in the soil existed mainly in the residual form (Pb_{re}), which accounted for 59.7% of the total Pb concentration. The proportion of Pb_{ex} decreased by 92.9 and 93.4% with GWB and PB application, and by 35.5 and 46.8% with Fe-GWB and Fe-PB application. Fe-GWB and Fe-PB increased the proportion of $Pb_{Fe\text{-}Mn}$ by 16.6 and 39.5%, respectively. For the proportion of Pb_{re}, only the PB treatment had significant impact, with an increase of 9.3%. Application of GWB and Fe-GWB increased the proportion of Pb_{or} by 38.42 and 82.8%, compared to the control. Besides, all biochar treatments apparently decreased the mobile fractions (sum of Pb_{ex} and Pb_{ca}) of Pb, and the pristine biochars were more effective than the Fe-engineered biochars (Fig. 5, Fig. S3). Overall, an increase of the Pb_{re}, and a decrease of the mobile fractions confirmed the stabilization of Pb caused by biochar amendments. Furthermore, PB exhibited higher efficacy in mitigating Pb contamination than GWB.

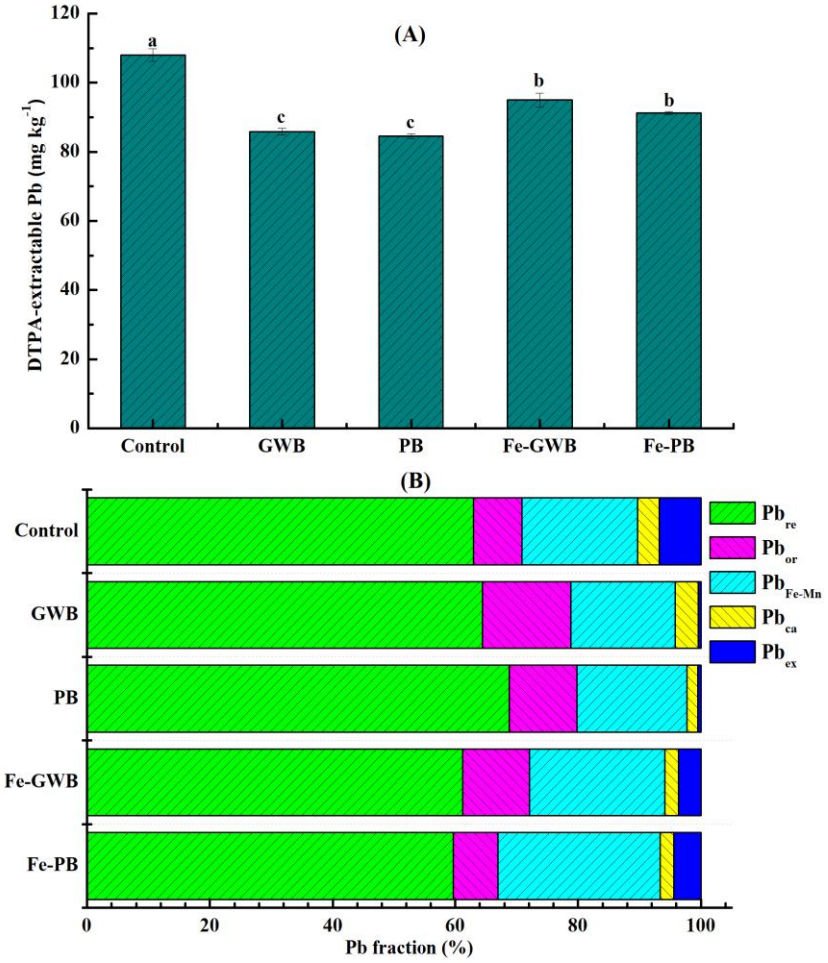

Fig. 5 Effect of pristine and iron-engineered biochar application on DTPA-extractable Pb (A), and redistribution of Pb (B) in soil. Treatments: green waste biochar (GWB), pig biochar (PB), iron-engineered green waste biochar (Fe-GWB), and iron-engineered pig biochar (Fe-PB). Pb fractionation: Exchangeable Pb (Pb_{ex}), carbonate bound Pb (Pb_{ca}), Fe-Mn oxide bound Pb (Pb_{Fe-Mn}), organic bound Pb (Pb_{or}), and residual Pb (Pb_{re}). Error bars are standard error of means (n=4). Different letters above bars indicate significant difference between treatments at $P<0.05$.

The pristine biochars were more effective in Pb immobilization and bioavailability reduction than the Fe-engineered biochars, which could be due to the following proposed mechanisms. First, the pristine biochar-induced increase of soil pH (Fig. 2A) could be the predominant factor affecting the Pb availability and redistribution. Li et al. (2020) reported that the addition of coconut fiber biochar increased the soil pH, as a result of which Pb^{2+} reacted with OH^- to form precipitation under alkaline conditions, and thus reducing Pb mobility in contaminated soils. A negative correlation ($P<0.05$) was found between soil pH and DTPA-extractable Pb (Fig. 4), suggesting that the soil pH could be considered as a crucial factor in influencing Pb mobilization in this study. The increased mobility and bioavailability of Pb after Fe-GWB and Fe-PB application might be linked to the decreased pH caused by these two Fe-engineered biochars (Fig. 2A). Second, the presence of mineral elements (e.g., P, Ca, K, Mg, and Na) generated from biochars in soil may contribute to Pb immobilization via cation exchange (Netherway et al., 2019). In the current study, the pristine biochars had higher CEC than the Fe-engineered biochars (Table 1), which provided an evidence that the pristine biochars might immobilize Pb through cation exchange mechanism. Third, surface complexation of Pb^{2+} with functional groups on biochar could be another possible mechanism. Wang et al. (2017) found that application of corn straw- and municipal sludge-derived biochars promoted the surface complexation reactions between Pb^{2+} and functional groups (e.g., -OH, -COOH, -CH, -C=O, C=C). In our study, higher abundance of functional groups on pristine biochars were detected, as compared to the Fe-engineered biochars (Fig. 1), which also supported the higher Pb immobilization efficiency of the pristine biochars due to the formation of complexes. Furthermore, it was likely that the anions (PO_4^{3-} or/and CO_3^{2-}) released from the pristine biochars, especially PB, might promote the immobilization of Pb in soil through formation of insoluble precipitates

(Netherway et al., 2019). Many studies pointed out that the relatively high efficiency of biochar in immobilizing Pb may be resulted from the precipitation between Pb^{2+} and phosphate (Ok et al., 2010; Ahmad et al., 2012). This was one of the reasons for the higher Pb immobilization when soil was treated with P-rich PB than with GWB. A significant negative correlation between the concentrations of DTPA-extractable Pb and Olsen P was observed in this study (Fig. 4), implying that Pb precipitation with phosphate was responsible for Pb immobilization.

3.5 Effect of biochars on gene abundance of bacteria and fungi

Application of biochar increased the bacterial 16S rRNA gene copy numbers in soil, by 40.1, 51.3, 33.8 and 46.8% for GWB, PB, Fe-GWB and Fe-PB, respectively, compared to the control (Fig. 6A). This could be attributed to the increased TOC content in the soil following the application of biochars (Fig. 2B), which provided essential C source to promote the growth and reproduction of bacterial population (Chen et al. 2013). The porous structure of biochar could provide a suitable habitat with abundant aeration and water for microorganisms protecting them from predators and harsh chemical conditions (Zhu et al., 2017; Tu et al., 2020). Pearson's correlation analysis showed a significant ($P<0.05$) negative correlation between bacterial 16S rRNA gene copy numbers, and DTPA-extractable Pb and $NH_4H_2PO_4$-extractable As (Fig. 4), indicating that the stress caused by As and Pb was a potential factor responsible for the decline of bacterial activities. The application of the pristine and Fe-engineered biochars mitigated the biotoxicity of As and Pb, and thus enhanced the bacterial abundance in the soil. Additionally, biochars supplied additional nutrients for the microorganisms, thereby promoting their growth and reproduction, in turn facilitating soil Pb immobilization.

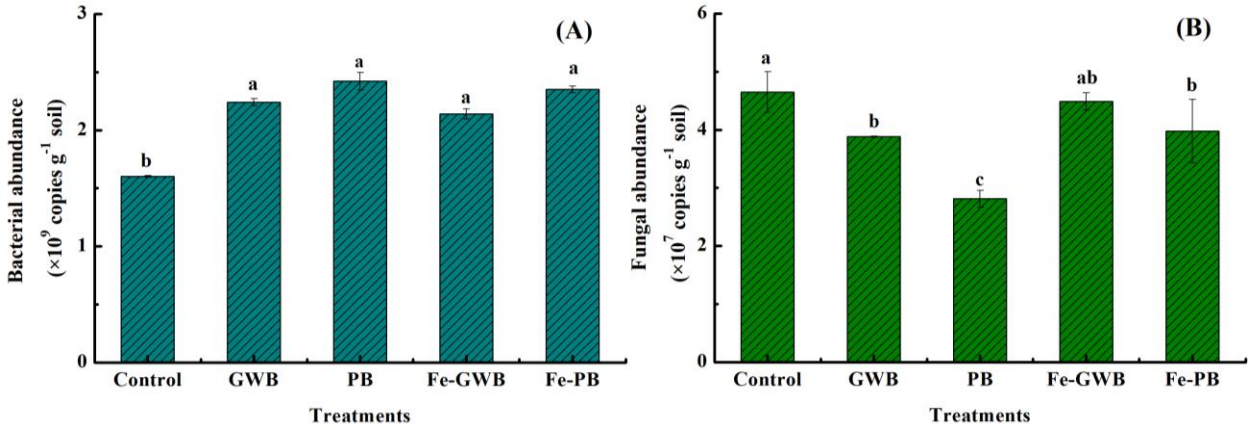

Fig. 6 Effect of pristine and iron-engineered biochar application on gene abundance of bacteria (A), and fungi (B). Treatments: green waste biochar (GWB), pig biochar (PB), iron-engineered green waste biochar (Fe-GWB), and iron-engineered pig biochar (Fe-PB). Error bars are standard error of means (n=4). Different letters above bars indicate significant difference between treatments at $P<0.05$.

The fungal 18S rRNA gene copy numbers decreased by 16.6 and 39.6% in the GWB and PB treatment, respectively (Fig. 6B). In the current study, the pH of soils treated with GWB and PB was significantly ($P<0.05$) higher than that of the control soil (Fig. 2A). As reported by Rousk et al. (2009), the increased pH of soil might have contributed to the decrease of fungal activity. However, although there was no significant difference between the pH of GWB and PB treatments (Fig. 2A), a significant ($P<0.05$) higher fungal abundance was observed in the GWB-treated soil as compared to the PB-treated soil. This result might be ascribed to the higher C content in GWB than that in PB. The extra C source for fungal growth might increase the buffer capacity of soil, thereby counteracting the effect of elevated pH. Overall, bacteria and fungi vary greatly in their properties, nutrient requirements and stress resistance, as well as their response to the environment, such as resilience to pH change and PTE stress (Rousk et al., 2009). Bacteria are more sensitive to labile substrates than fungi (Lehmann et al., 2011). Therefore, bacteria are more receptive to the labile C supplied with biochar, thereby affected more than fungi (Farrell et al., 2013).

4. Conclusions

This study showed that the Fe-loading to pristine biochars decreased the pH, surface alkalinity, SSA, and functional groups, but increased the ash content in the engineered biochars. Following application to a contaminated soil, Fe-engineered biochars reduced the soil pH, and improved the TOC content. Both pristine and Fe-engineered biochars decreased the bioavailability of Pb in the soil, and pristine biochars performed more effective than Fe-engineered biochars, whereas only the Fe-engineered biochars decreased potentially available soil As. The (im)mobilization of As and Pb by the pristine and Fe-engineered biochars was selective, and varied with the elemental characteristics. Sequential chemical extraction results suggested that the application of biochars accelerated the transformation of As and Pb from labile to relatively stable forms. The Fe-engineered biochars could effectively transform the labile form of As to relatively stable forms, while the pristine biochars could effectively transform the labile form of Pb to relatively stable forms. Biochar-induced enhancement of bacterial abundance indicated that biochar application mitigated the ecotoxic stress of As and Pb, and improved the soil quality. These findings suggested that biochar could be used as eco-friendly biosorbents not only by decreasing the mobility of As and Pb in soils, but by encouraging the recycling of animal and plant derived wastes.

Acknowledgements

This study was financially supported by the National Natural Science Foundation of China (Grant No. 21876027), and the Special Fund for the Science and Technology Innovation Team of Foshan, China (Grant No. 1920001000083).

References

Ahmad, M., Soo Lee, S., Yang, J.E., Ro, H.M., Han Lee, Y., Sik Ok, Y., 2012. Effects of soil dilution and amendments (mussel shell, cow bone, and biochar) on Pb availability and phytotoxicity in military shooting range soil. Ecotox. Environ. Saf. 79, 225-231.

Amen, R., Bashir, H., Bibi, I., Shaheen, S.M., Niazi, N.K., Shahid, M., Hussain, M.M., Antoniadis, V., Shakoor, M.B., Al-Solaimani, S.G., Wang, H., Bundschuh, J., Rinklebe, J., 2020. A critical review on arsenic removal from water using biochar-based sorbents: The significance of modification and redox reactions. Chem. Eng. J. 396, 125195.

Antoniadis, V., Levizou, E., Shaheen, S.M., Ok, Y.S., Sebastian, A., Baum, C., Prasad, M.N.V., Wenzel, W.W., Rinklebe, J., 2017. Trace elements in the soil-plant interface: Phytoavailability, translocation, and phytoremediation–A review. Earth Sci. Rev. 171, 621-645.

Bandara, T., Franks, A., Xu, J., Bolan, N., Wang, H., Tang, C., 2020. Chemical and biological immobilization mechanisms of potentially toxic elements in biochar-amended soils. Crit. Rev. Environ. Sci. Technol. 50, 903-978.

Beiyuan, J., Awad, Y.M., Beckers, F., Wang, J., Tsang, D.C.W., Ok, Y.S., Wang, S.-L., Wang, H., Rinklebe, J., 2020. (Im)mobilization and speciation of lead under dynamic redox conditions in a contaminated soil amended with pine sawdust biochar. Environ. Inter. 135, 105376.

Bolan, N., Mahimairaja, S., Kunhikrishnan, A., Naidu, R., 2013. Sorption-bioavailability nexus of arsenic and cadmium in variable-charge soils. J. Hazard. Mater. 261, 725-732.

Chen, H., Yang, X., Wang, H., Sarkar, B., Shaheen, S.M., Gielen, G., Bolan, N., Guo, J., Che, L., Sun, H., Rinklebe, J., 2020. Animal carcass- and wood-derived biochars improved nutrient bioavailability, enzyme activity, and plant growth in metal-phthalic acid ester co-contaminated soils: A trial for reclamation and improvement of degraded soils. J. Environ. Manage. 261, 110246.

Chen, J., Liu, X., Zheng, J., Zhang, B., Yu, X., 2013. Biochar soil amendment increased bacterial but decreased fungal gene abundance with shifts in community structure in a slightly acid rice paddy from Southwest China. Appl. Soil Ecol. 71, 33–44.

Dong, S., Xu, W., Wu, F., Yan, C., Li, D., Jia, H., 2016. Fe-modified biochar improving transformation of arsenic from in soil and inhibiting its absorption of plant. Transactions of the Chinese Society of Agricultural Engineering 32, 204-212.

El-Naggar, A., Lee, M.-H., Hur, J., Lee, Y.H., Igalavithana, A.D., Shaheen, S.M., Ryu, C., Rinklebe, J., Tsang, D.C.W., Ok, Y.S., 2020. Biochar-induced metal immobilization and soil biogeochemical process: An integrated mechanistic approach. Sci. Total Environ. 698, 134112.

Fang, Q., Chen, B., Lin, Y., Guan, Y., 2014. Aromatic and hydrophobic surfaces of wood-derived biochar enhance perchlorate adsorption via hydrogen bonding to oxygen-containing organic groups. Environ. Sci. Technol. 48, 279-288.

Fang, Z., Gao, Y., Bolan, N., Shaheen, S.M., Xu, S., Wu, X., Xu, X., Hu, H., Lin, J., Zhang, F., Li, J., Rinklebe, J., Wang, H., 2020. Conversion of biological solid waste to graphene-containing biochar for water remediation: A critical review. Chem. Eng. J. 390, 124611.

Farrell, M., Kuhn, T.K., Macdonald, L.M., Maddern, T.M., Murphy, D.V., Hall, P.A., Singh, B.P., Baumann, K., Krull, E.S., Baldock, J.A., 2013. Microbial utilisation of biochar-derived carbon. Sci. Total Environ. 465, 288-297.

Fierer, N., Jackson, J.A., Vilgalys, R., Jackson, R.B., 2005. Assessment of soil microbial community structure by use of taxon-specific quantitative PCR assays. Appl. Environ. Microbiol. 71, 4117-4120.

Han, Y.S., Park, J.H., Kim, S.J., Jeong, H.Y., 2019. Redox transformation of soil minerals and arsenic in arsenic-contaminated soil under cycling redox conditions. J. Hazard. Mater. 378, 120745.

Karczewska, A., Lewińska, K., Siepak, M., Gałka, B., Dradrach, A., Szopka, K., 2018. Transformation of beech forest litter as a factor that triggers arsenic solubility in soils developed on historical mine dumps. J. Soils Sediments 18, 2749-2758.

Komarek, M., Vanek, A., Ettler, V., 2013. Chemical stabilization of metals and arsenic in contaminated soils using oxides - a review. Environ. Pollut. 172, 9-22.

Kwon, G., Bhatnagar, A., Wang, H., Kwon, E.E., Song, H., 2020. A review of recent advancements in utilization of biomass and industrial wastes into engineered biochar. J. Hazard. Mater. 400, 123242.

Lehmann, J., Rillig, M.C., Thies, J., Masiello, C.A., Hockaday, W.C., Crowley, D., 2011. Biochar effects on soil biota- a review. Soil Biol. Biochem. 43, 1812-1836.

Li, J., Wang, S.-L., Zhang, J., Zheng, L., Chen, D., Wu, Z., Shaheen, S.M., Rinklebe, J., Ok, Y.S., Wang, H., Wu, W., 2020. Coconut-fiber biochar reduced the bioavailability of lead but increased its translocation rate in rice plants: Elucidation of immobilization mechanisms and significance of iron plaque barrier on roots using spectroscopic techniques. J. Hazard. Mater. 389, 122117.

Li, J., Zheng, L., Wang, S.-L., Wu, Z., Wu, W., Niazi, N.K., Shaheen, S.M., Rinklebe, J., Bolan, N., Ok, Y.S., Wang, H., 2019. Sorption mechanisms of lead on silicon-rich biochar in aqueous solution: Spectroscopic investigation. Sci. Total Environ. 672, 572-582.

Lindsay, W.L., Norvel, W. A., 1978. Development of a DTPA soil test for zinc, iron, manganese, and copper. Soil Sci. Soc Am J. 42, 421-428.

Lu, K., Yang, X., Gielen, G., Bolan, N., Ok, Y.S., Niazi, N.K., Xu, S., Yuan, G., Chen, X., Zhang, X., Liu, D., Song, Z., Liu, X., Wang, H., 2017. Effect of bamboo and rice straw biochars on the mobility and redistribution of heavy metals (Cd, Cu, Pb and Zn) in contaminated soil. J. Environ. Manage. 186, 285-292.

Lu, K., Yang, X., Shen, J., Robinson, B., Huang, H., Liu, D., Bolan, N., Pei, J., Wang, H., 2014. Effect of bamboo and rice straw biochars on the bioavailability of Cd, Cu, Pb and Zn to *Sedum plumbizincicola*. Agric. Ecosyst. Environ. 191, 124-132.

Lu, H.P., Li, Z.A., Gascó, G., Méndez, A., Shen, Y., Paz-Ferreiro, J., 2018. Use of magnetic biochars for the immobilization of heavy metals in a multi-contaminated soil. Sci. Total Environ. 622-623, 892-899.

Lu, L., Yu, W., Wang, Y., Zhang, K., Zhu, X., Zhang, Y., Wu, Y., Ullah, H., Xiao, X., Chen, B., 2020. Application of biochar-based materials in environmental remediation: from multi-level structures to specific devices. Biochar 2, 1-31.

May, L.A., Smiley, B., Schmidt, M.G., 2001. Comparative denaturing gradient gel electrophoresis analysis of fungal communities associated with whole plant corn silage. Can. J. Microbiol. 47, 829-841.

Netherway, P., Reichman, S., Laidlaw, M., Scheckel, K., Pingitore, N., Gascó, G., Méndez, A., Surapaneni, A., Paz-Ferreiro, J., 2019. Phosphorus-rich biochars can transform lead in an urban contaminated soil. J. Environ. Qual. 48(4), 1091-1099.

Nie, C., Yang, X., Niazi, N.K., Xu, X., Wen, Y., Rinklebe, J., Ok, Y.S., Xu, S., Wang, H., 2018. Impact of sugarcane bagasse-derived biochar on heavy metal availability and microbial activity: A field study. Chemosphere 200, 274-282.

Ok, Y.S., Oh, S.-E., Ahmad, M., Hyun, S., Kim, K.-R., Moon, D.H., Lee, S.S., Lim, K.J., Jeon, W.-T., Yang, J.E., 2010. Effects of natural and calcined oyster shells on Cd and Pb immobilization in contaminated soils. Environ. Earth Sci. 61, 1301-1308.

Palansooriya, K.N., Shaheen, S.M., Chen, S.S., Tsang, D.C.W., Hashimoto, Y., Hou, D., Bolan , N.B., Rinklebe, J., Yong, Y.S., 2020. Soil amendments for immobilization of potentially toxic elements in contaminated soils: A critical review. Environ Int. 134, 105046.

Panahi, H., Dehhaghi, M., Ok, Y.S., Nizami, A.-S., Khoshnevisan, B., Mussatto, S.I., Aghbashlo, M., Tabatabaei, M., Lam, S.S., 2020. A comprehensive review of engineered biochar: Production, characteristics, and environmental applications. J. Clean. Prod. 270, 122462.

Qiao, J., Yu, H., Wang, X., Li, F., Wang, Q., Yuan, Y., Liu, C., 2019. The applicability of biochar and zero-valent iron for the mitigation of arsenic and cadmium contamination in an alkaline paddy soil. Biochar 1, 203-212.

Rinklebe, J., Shaheen, S.M., El-Naggar, A., Wang, H., Du Laing, G., Alessi, D.S., Ok, Y.S., 2020. Redox-induced mobilization of Ag, Sb, Sn, and Tl in the dissolved, colloidal and solid phase of a biochar-treated and un-treated mining soil. Environ. Inter. 140, 105754.

Rousk, J., Brookes, P.C., Baath, E., 2009. Contrasting soil pH effects on fungal and bacterial growth suggest functional redundancy in carbon mineralization. Appl. Environ. Microbiol. 75, 1589-1596.

Shaheen, S.M., Niazi, N.K., Hassan, N.E.E., Bibi, I., Wang, H., Tsang , D.C.W., Ok, Y.S., Bolan, N., Rinklebe, J., 2019. Wood-based biochar for the removal of potentially toxic elements in water and wastewater: a critical review. Int. Mater. Rev. 64(4), 216-247.

Shaheen, S.M., Kwon, E.E., Biswas, J.K., Tack, F.M.G., Ok, Y.S., Rinklebe, J. 2017. Arsenic, chromium, molybdenum, and selenium: Geochemical fractions and potential mobilization in riverine soil profiles originating from Germany and Egypt. Chemosphere 180, 553-563.

Tang, X., Shen, H., Chen, M., Yang, X., Yang, D., Wang, F., Chen, Z., Liu, X., Wang, H., Xu, J., 2020. Achieving the safe use of Cd- and As-contaminated agricultural land with an Fe-based biochar: A field study. Sci. Total Environ. 706, 135898.

Tessier, A., Campbell, P.G.C., Bisson, M., 1979. Sequential extraction procedure for the speciation of particulate trace metals. Anal. Chem.

Tu, C., Wei, J., Guan, F., Liu, Y., Sun, Y., Luo, Y., 2020. Biochar and bacteria inoculated biochar enhanced Cd and Cu immobilization and enzymatic activity in a polluted soil. Environ. Int. 137, 105576.

Wan, X., Li, C., Parikh, S.J., 2020. Simultaneous removal of arsenic, cadmium, and lead from soil by iron-modified magnetic biochar. Environ. Pollut. 261, 114157.

Wang, L., Ok, Y.S., Tsang, D.C.W., Alessi, D.S., Rinklebe, J., Wang, H., Mašek, O., Hou, R., O'Connor, D., Hou, D., 2020. New trends in biochar pyrolysis and modification strategies: feedstock, pyrolysis conditions, sustainability concerns and implications for soil amendment. Soil Use Manage. 36, 358-386.

Wang, S., Guo, W., Gao, F., Yang, R., 2017. Characterization and Pb(II) removal potential of corn straw- and municipal sludge-derived biochars. Roy. Soc. Open Sci. 4(9), 170402.

Wenzel, W.W., Kirchbaumer, N., Prohaska, T., Stingeder, G., Adriano, D.C., 2001. Arsenic fractionation in soils using an improved sequential extraction procedure. Anal. Chim. Acta 436, 309-323.

Wu, P., Wang, Z., Wang, H., Bolan, N.S., Wang, Y., Chen, W., 2020. Visualizing the emerging trends of biochar research and applications in 2019: a scientometric analysis and review. Biochar 2, 135-150.

Wu, W., Yang, M., Feng, Q., McGrouther, K., Wang, H., Lu, H., Chen, Y., 2012. Chemical characterization of rice straw-derived biochar for soil amendment. Biomass Bioenergy 47, 268-276.

Xia, S., Song, Z., Jeyakumar, P., Shaheen, S.M., Rinklebe, J., Ok, Y.S., Bolan, N., Wang, H., 2019. A critical review on bioremediation technologies for Cr(VI)-contaminated soils and wastewater. Crit. Rev. Environ. Sci. Technol. 49, 1027-1078.

Xing, Y., Wang, J., Shaheen, S. M., Feng, X., Chen, Z., Zhang, H., Rinklebe, J., 2019. Mitigation of mercury accumulation in rice using rice hull-derived biochar as soil amendment: A field investigation. J. Hazard. Mater. 388, 121747.

Xu, X., Liu, Y., Singh, B.P., Yang, Q., Zhang, Q., Wang, H., Xia, Z., Di, H., Brajesh, K., Xu, J., Li, Y., 2020. NosZ clade II rather than clade I determine in situ N2O emissions with different fertilizer types under simulated climate change and its legacy. Soil Biol. Biochem. 150, 107974.

Xu, X., Xia, Z., Liu, Y., Liu, E., Müller, K., Wang, H., Luo, J., Wu, X., Bei, Y., Fang, Z., Xu, J., Di, H., Li, Y., 2021. Interactions between methanotrophs and ammonia oxidizers modulate the response of in situ methane emissions to simulated climate change and its legacy in an acidic soil. Sci. Total Environ. 752, 142225.

Xu, Y., Seshadri, B., Sarkar, B., Wang, H., Rumpel, C., Sparks, D., Farrell, M., Hall, T., Yang, X., Bolan, N., 2018. Biochar modulates heavy metal toxicity and improves microbial carbon use efficiency in soil. Sci. Total Environ. 621, 148-159.

Yang, X., Liu, J., McGrouther, K., Huang, H., Lu, K., Guo, X., He, L., Lin, X., Che, L., Ye, Z., Wang, H., 2016. Effect of biochar on the extractability of heavy metals (Cd, Cu, Pb, and Zn) and enzyme activity in soil. Environ. Sci. Pollut. Res. 23, 974-984.

Yang, X., Lu, K., Mcgrouther, K., Che, L., Hu, G., Wang, Q., Liu, X., Shen, L., Huang, H., Ye, Z., Wang, H., 2017. Bioavailability of Cd and Zn in soils treated with biochars derived from tobacco stalk and dead pigs. J. Soils Sediments 17, 751-762.

Yin, D., Wang, X., Peng, B., Tan, C., Ma, L.Q., 2017. Effect of biochar and Fe-biochar on Cd and As mobility and transfer in soil-rice system. Chemosphere 186, 928-937.

Yin, G., Song, X., Tao, L., Sarkar, B., Sarmah, A.K., Zhang, W., Lin, Q., Xiao, R., Liu, Q., Wang, H., 2020. Novel Fe-Mn binary oxide-biochar as an adsorbent for removing Cd(II) from aqueous solutions. Chem. Eng. J. 389, 124465.

Zeng, X., Wu, P., Su, S., Bai, L., Feng, Q., 2012. Phosphate has a differential influence on arsenate adsorption by soils with different properties. Plant Soil Environ. 58, 405-411.

Zhu, X., Chen, B., Zhu, L., Xing, B., 2017. Effects and mechanisms of biochar-microbe interactions in soil improvement and pollution remediation: A review. Environ. Pollut. 227, 98-115.

Supplementary material

Table S1 Effect of pristine and iron-engineered biochars on Olsen-P and DTPA-extractable Fe in soil.

Treatments	Control	GWB	PB	Fe-GWB	Fe-PB
Olsen P (mg kg^{-1})	2.05±0.12c	3.26±0.15b	11.97±1.42a	3.97±0.10b	3.96±0.33b
DTPA-extractable Fe (mg kg^{-1})	151.07±2.54bc	88.70±10.10a	149.44±3.93bc	147.79±5.84b	178.68±3.97c

Treatments: control, pristine green waste biochar (GWB), pristine pig biochar (PB), iron-engineered green waste biochar (Fe-GWB) and iron-engineered pig biochar (Fe-PB). Different letters indicate significant differences between treatments at $P<0.05$ level.

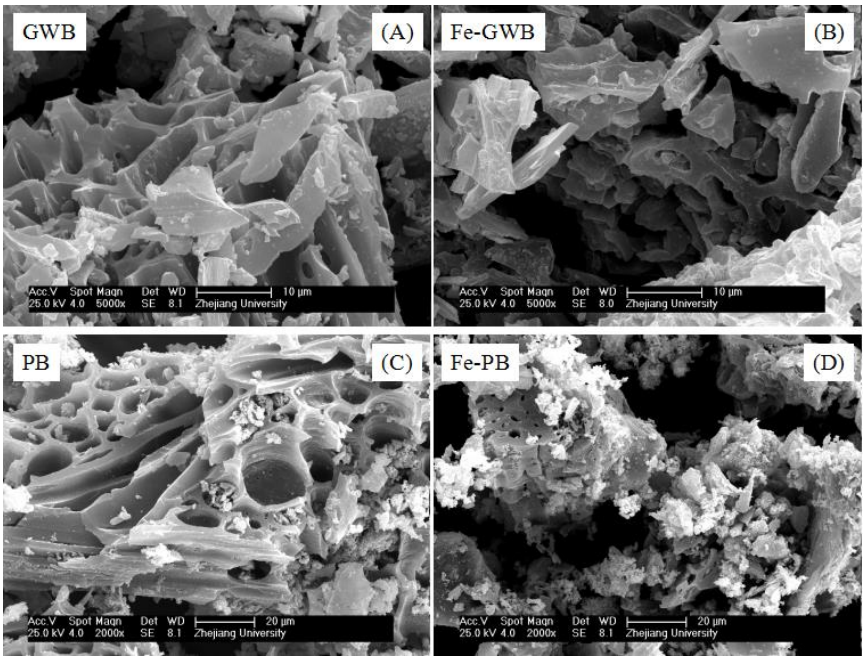

Fig. S1 Scanning electron microscope (SEM) images of pristine green waste biochar (GWB) (A), iron-engineered green waste biochar (Fe-GWB) (B), pristine pig biochar (PB) (C), and iron-engineered pig biochar (Fe-PB) (D).

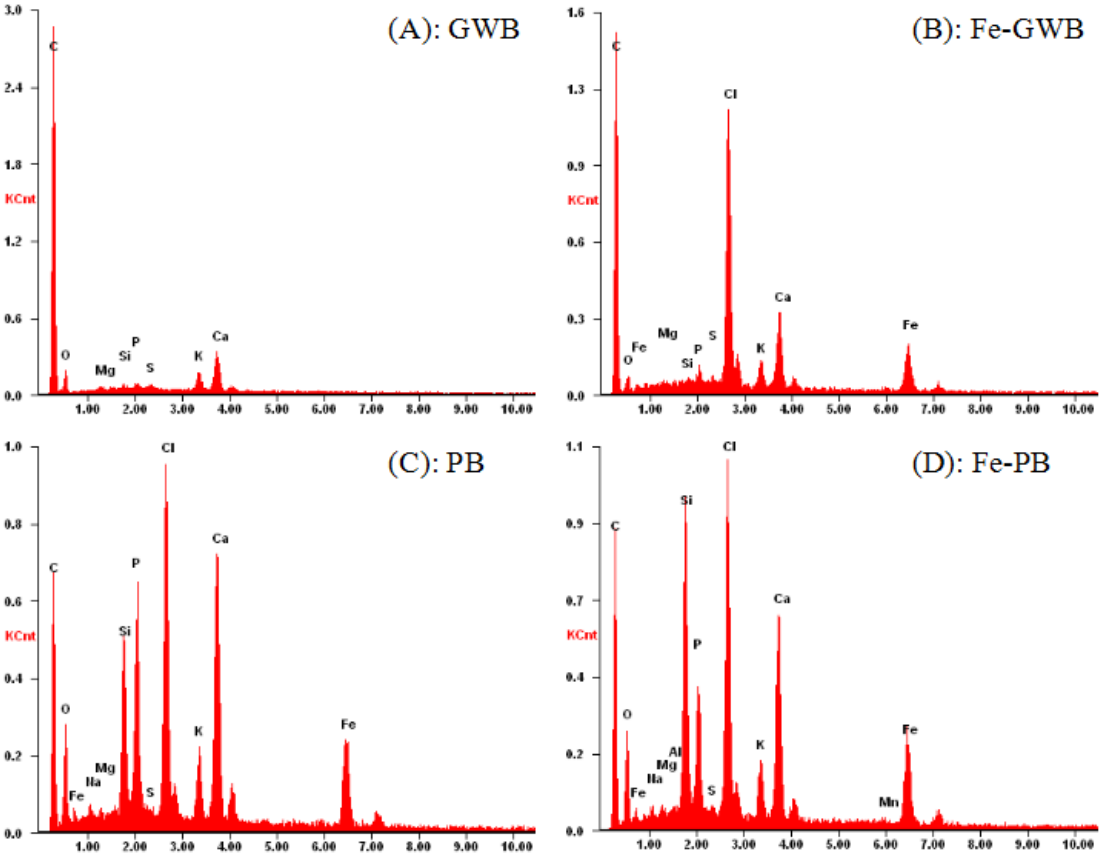

Fig. S2. Energy dispersive X-ray spectrometry (EDS) of pristine green waste biochar (GWB) (A), iron-engineered green waste biochar (Fe-GWB) (B), pristine pig biochar (PB) (C), and iron-engineered pig biochar (Fe-PB) (D).

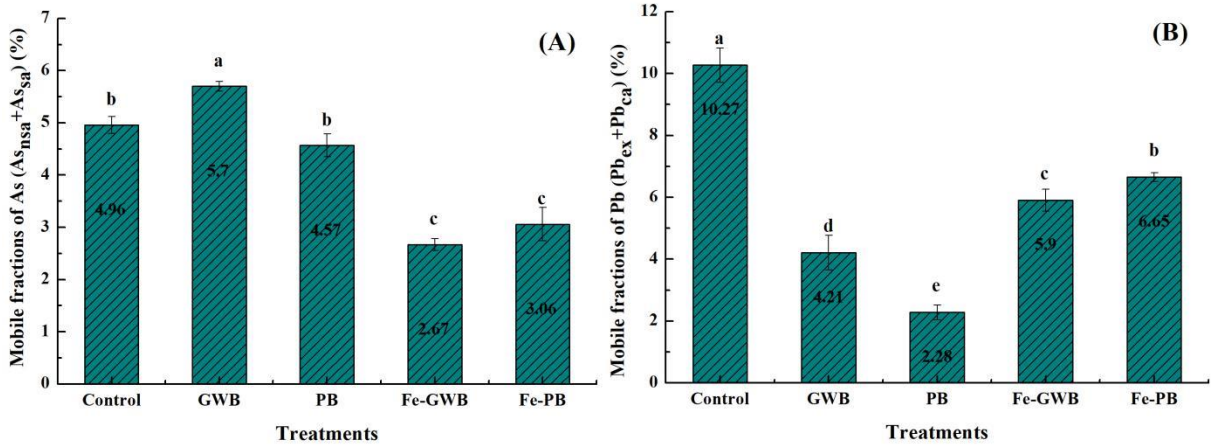

Fig. S3. Mobile fractions of As and Pb. Mobile fractions of As (As_{nsa} + As_{sa}) (A). Mobile fractions of Pb (Pb_{ex} + Pb_{ca}) (B).